Comparison of Motion Correction Methods Incorporating Motion Modelling for PET/CT Using a Single Breath Hold Attenuation Map

Alexander C. Whitehead * †, Ander Biguri *, Kuan-Hao Su ‡, Scott D. Wollenweber ‡, Charles W. Stearns ‡,
Brian F. Hutton *, Jamie R. McClelland † and Kris Thielemans * †

* Institute of Nuclear Medicine, University College London, UK   † Centre for Medical Image Computing,
University College London, UK   ‡ Molecular Imaging and Computed Tomography Engineering, GE Healthcare,
USA

Abstract—**Introducing motion models into respiratory motion correction methods can lead to a reduction in blurring and artefacts. However, the pool of research where motion modelling methods are applied to combined positron emission tomography and computed tomography is relatively shallow. Previous work used non-attenuation corrected time-of-flight data to fit motion models, not only to motion correct the volumes themselves, but also to warp a single attenuation map to the positions of the initial gated data. This work seeks to extend previous work to offer a comparison of respiratory motion correction methods, not only with and without motion models, but also to compare pair-wise and group-wise registration techniques, on simulation data, in a low count scenario, where the attenuation map is from a pseudo-breath hold acquisition. To test the methods, 4-Dimensional Extended Cardiac Torso images are constructed, simulated and reconstructed without attenuation correction, then motion corrected using one of pair-wise, pair-wise with motion model, group-wise and group-wise with motion model registration. Next these motion corrected volumes are registered to the breath hold attenuation map. The positron emission tomography data are then reconstructed using deformed attenuation maps and motion corrected. Evaluation compares the results of these methods against non-motion corrected and motion free examples. Results indicate that the incorporation of motion models and group-wise registration, improves contrast and quantification.**

I. INTRODUCTION

MOTION modelling is a Motion Correction (MC) technique, where time- or gate-dependence of Deformation Vector Fields (DVFs) are parameterised in terms of a Surrogate Signal (SS) [1]. Motion Models (MMs) attempt to improve upon solely registering data, being more robust to noise, but also allow for the correction of unseen data. It has shown good promise in Computed Tomography (CT) [2], Magnetic Resonance (MR) [3] and combined Positron Emission Tomography (PET)/MR [4], but has not yet seen widespread adoption in clinical PET, where PET/CT is far more common.

Respiratory Motion (RM) reduces resolution and degrades the accuracy of quantification in PET by introducing blurring to the PET volume and also misalignment between the PET and CT [5]. Most existing MC methods rely on pair-wise registration of gated PET volumes, this is a challenging problem due to the low contrast and high noise [6]. Respiratory MC is an ideal problem area for the application of MMs as SSs are already commonly available from respiratory gating, such as acquired by Real Time Position Management (RPM) or Principal Component Analysis (PCA) [7].

In previous work, the possibility of using MMs to MC Non-Attenuation Corrected (NAC) Time-of-Flight (TOF) PET, and warp a Attenuation Map (Mu-Map) from a position close to the mean respiratory position to each gate, was investigated. It was found that the combination of both the MM and TOF was sufficient to perform an Attenuation Corrected (AC) reconstruction with MC, without introducing artefacts, while increasing resolution and quantification accuracy [8], [9]. This work seeks to extend the method further through the use of a more modular framework, which allows for the fair comparison of different registration methods, both with and without MMs. Furthermore, this work uses more realistic simulation and count levels, compared to previous work (where more simple registration methods would fail). Additionally, this work strives to improve the Mu-Map warping aspect of the previous method, by fixing the Mu-Map at end inhalation (as opposed to the mean respiratory position). This is more clinically relevant but also challenging.

A method incorporating MMs for dynamic PET/CT, was proposed and tested on clinical data in [10]. The work presented here, differentiates itself by firstly using a 2-Dimensional (2D) SS, rather than a 1-Dimensional (1D) SS, thus both inter- and intra-gate motion can be included in the model, at the expense that each gate contains fewer counts. Additionally, the group-wise method, presented here, makes use of an iterative MC algorithm rather than using only a pair-wise method.

II. METHODS

A. XCAT Volume Generation

4-Dimensional Extended Cardiac Torso (XCAT) [11] was used to generate 240 volumes over a 120 s period using

a respiratory trace, derived from MR navigator patient data. The max displacement of Anterior Posterior and Superior Inferior motion, was set to $1.2\,\mathrm{cm}$ and $2.0\,\mathrm{cm}$ respectively. Activity concentrations were derived from a static Fluorine-18 Fludeoxyglucose (18F-FDG) patient scan. The Field Of View (FOV) included the base of the lungs, diaphragm and the top of the liver with a $20\,\mathrm{mm}$ diameter spherical lesion (smaller than the max displacement, due to RM) was placed into the base of the right lung (within the max displacement, due to RM, of the diaphragm).

B. PET Acquisition Simulation and Non-Attenuation Corrected Image Reconstruction

PET acquisitions were simulated (and reconstructed) using Software for Tomographic Image Reconstruction (STIR) [12], [13] through Synergistic Image Reconstruction Framework (SIRF) [14], to forward project data using the geometry of a General Electric (GE) Discovery 710, but using a TOF resolution of $375\,\mathrm{ps}$. This TOF resolution is higher than that of the 710, but is closer to the newer GE Signa PET/MR system. TOF mashing was used to reduce computation time resulting in 13 TOF bins of size $376.5\,\mathrm{ps}$. Attenuation was included using the relevant Mu-Maps generated by XCAT. Pseudo-randoms and scatter were added. Randoms were added by summing the scaled mean value to each voxel of each volume prior to forward projection. Pseudo scatter was added by summing the scaled and smoothed mean Mu-Map prior to forward projection, the smoothing parameter was optimised to give scatter which tapered at the same rate as in clinical data. A full scatter simulation was not performed due to software limitations.

Noise was simulated, such that data matched an acquisition over $120\,\mathrm{s}$, emulating a standard single bed position acquisition. The count rate was selected to match that of research scans, i.e. below that of diagnostic clinical scans. This count rate was selected as a 'worst case scenario'.

A respiratory SS was generated using PCA [7]. The magnitude of this signal and its gradient, was used to gate data into 30 respiratory bins using displacement gating (10 amplitude and 3 gradient bins). Gates with fewer than 0.42% of the counts were discarded. For the purpose of the MM fitting, SS values were determined for the post-gated data by taking an average of the SS values of data in each bin.

Data were reconstructed, without AC, using Ordered Subset Expectation Maximisation (OSEM) with two full iterations and 24 subsets [15].

C. Registration

Before being registered, each volume underwent pre-processing. Including replication of end-slices, transformation to be approximately normally distributed [16] and post-smoothing. This pre-processing was only applied to intermediate data and was not used for the final output of the method.

Two registration methods were examined in this work. Firstly, pair-wise registration, where the reference position was selected as the gate with the highest number of counts. All other gates were registered to it. Secondly, group-wise registration, where after an initial pair-wise registration step, the DVFs generated

had the inverse mean of all DVFs composed with them, before a new reference volume was resampled. Registration to the new reference volume, followed by the inverse mean composition and resample, continued for a set number of iterations. NiftyReg [17] was used to perform registrations using a B-spline parameterisation. The Gaussian smoothing Full Width at Half Maximum (FWHM), Control Point Grid spacing of the B-spline coefficients, Bending Energy regularisation term weight and number of iterations were tuned using a grid search.

D. Motion Model Estimation

If a MM was used, then it was fit as a direct Respiratory Correspondence Model on the DVFs from Section II-C and the SS from Section II-B. A weighted Linear Regression was used, where the weighting was taken based on the number of counts in each gate. Once a MM was fit, new DVFs were generated for each gate, using the SS values used to fit the MM. For group-wise registration, MM fitting occurred between iterations, the DVFs generated by the MM were used to resample the new target volume at each iteration.

E. Attenuation Map Warping

A Mu-Map at end inhalation was selected from the Mu-Maps generated by XCAT. The PET volume from the previous step was then registered to this Mu-Map, and the resulting DVFs were composed with the DVFs from the last iteration of the MC method, and a new volume resampled. The inverse of these DVFs, were then used to warp the Mu-Map to each gate.

F. Motion Corrected Image Reconstruction with AC

Data were re-reconstructed with AC, using the Mu-Maps from Section II-E. The same reconstruction parameters as in Section II-F were used. MC was then applied to data following Section II-C, Section II-D and Section II-E. Volumes were post-filtered using a Gaussian smoothing, with a FWHM of $6.39\,\mathrm{mm}$ in the transverse plane (equivalent to three voxels) and $3.27\,\mathrm{mm}$ (equivalent to one voxel) in the axial direction.

G. Evaluation

In addition to the reconstructions performed in Section II-F, data were also reconstructed without MC, using either a sum of all Mu-Maps (to emulate an Averaged CINE-CT (AV-CCT)), or the end inhalation Mu-Map. For the present evaluation, the volumes without MC were registered to the position of the end inhalation Mu-Map. Additionally, DVFs generated by each method were also applied to noiseless data for visual analysis.

Comparisons used included: A profile over the lesion, Standard Uptake Value $\mathrm{(SUV)_{max}}$ and $\mathrm{SUV_{peak}}$ (defined following European Association of Nuclear Medicine (EANM) guidelines [18]).

III. RESULTS

A visual comparison of the reconstructed images (see Fig. 1) shows that more blurring can be seen at the boundary between
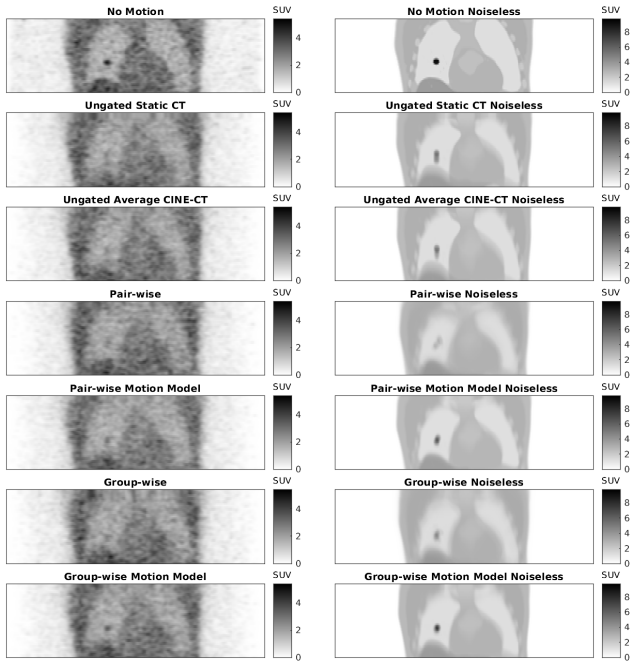
Fig. 1. First column contains AC MC reconstructions and the second column contains the result of applying the final MC on the original XCAT images (for easier assessment of the accuracy of the estimated DVFs); ungated static CT, ungated AV-CCT, pair-wise, pair-wise MM, group-wise, group-wise MM. Colour map ranges are consistent for all images in each column.
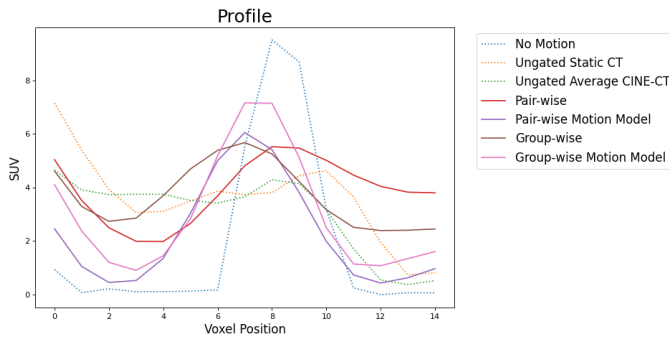

Fig. 2. A profile across the lesion for; ungated static CT, ungated AV-CCT, pair-wise, pair-wise MM, group-wise, group-wise MM.

TABLE I
COMPARISON OF SUV_{MAX} AND SUV_{PEAK} BETWEEN: UNGATED STATIC CT, UNGATED AV-CCT, PAIR-WISE, PAIR-WISE MM, GROUP-WISE, GROUP-WISE MM.

SUV	Max	Peak
No Motion	9.50	9.06
Ungated Static CT	5.25	5.15
Ungated AV-CCT	5.38	5.07
Pair-wise	4.21	3.92
Pair-wise MM	6.63	6.07
Group-wise	4.42	4.21
Group-wise MM	7.64	7.03

the diaphragm and lung for the MM free methods. Additionally, where a MM was used, the lesion appears to be more homogeneous.

The peak of the profile (see Fig. 2) is greater for MM methods than for MM free methods. However, the peaks for all MC methods are greater than ungated methods.

SUV results consistently show that including MMs increases the SUV when compared to when one is not used (see TABLE I).

IV. DISCUSSION AND CONCLUSIONS

Results from a visual analysis, a comparison of profiles and SUV, show that adding a MM to any MC method (tested here) improved the quality of volumes produced. Although, from a visual analysis volumes appear preferable with any MC method, quantitative evaluation points to the conclusion that for MC to be successful, for very noisy data, MMs are required in practice.

In the future, work will focus on incorporating the methods presented here into an iterative Image Registration and MC method and tested on patient data from several research studies.

REFERENCES

[1] J. R. McClelland *et al.*, "Respiratory motion models: A review," *Medical Image Analysis*, vol. 17, no. 1, pp. 19–42, Jan. 2013.

[2] T. Li *et al.*, "Enhanced 4D cone-beam CT with inter-phase motion model," *Medical Physics*, vol. 34, no. 9, pp. 3688–3695, Aug. 2007.

[3] D. Manke *et al.*, "Respiratory motion in coronary magnetic resonance angiography: A comparison of different motion models," *Journal of Magnetic Resonance Imaging*, vol. 15, no. 6, pp. 661–671, Jun. 2002.

[4] R. Manber *et al.*, "Joint PET-MR respiratory motion models for clinical PET motion correction.," *Physics in medicine and biology*, vol. 61, no. 17, pp. 6515–30, Sep. 2016.

[5] S. A. Nehmeh *et al.*, "Respiratory Motion in Positron Emission Tomography/Computed Tomography: A Review," *Seminars in Nuclear Medicine*, vol. 38, no. 3, pp. 167–176, May 2008.

[6] F. P. Oliveira *et al.*, "Medical image registration: a review," *Computer Methods in Biomechanics and Biomedical Engineering*, vol. 17, no. 2, pp. 73–93, Jan. 2014.

[7] K. Thielemans *et al.*, "Device-less gating for PET/CT using PCA," in *IEEE NSS-MIC*, IEEE, 2011.

[8] A. C. Whitehead *et al.*, "Impact of Time-of-Flight on Respiratory MotionModelling using Non-Attenuation-Corrected PET," in *IEEE NSS-MIC*, IEEE, 2019.

[9] A. C. Whitehead *et al.*, "PET/CT Respiratory Motion Correction With a Single Attenuation Map Using NAC Derived Deformation Fields," in *IEEE NSS-MIC*, IEEE, 2020.

[10] C. Chan *et al.*, "Non-Rigid Event-by-Event Continuous Respiratory Motion Compensated List-Mode Reconstruction for PET," *IEEE Transactions on Medical Imaging*, vol. 37, no. 2, pp. 504–515, Feb. 2018.

[11] W. P. Segars *et al.*, "4D XCAT phantom for multimodality imaging research," *Medical Physics*, vol. 37, no. 9, pp. 4902–4915, Aug. 2010.

[12] K. Thielemans *et al.*, "STIR: software for tomographic image reconstruction release 2," *Physics in Medicine and Biology*, vol. 57, no. 4, pp. 867–883, Feb. 2012.

[13] N. Efthimiou *et al.*, "Implementation and validation of time-of-flight PET image reconstruction module for listmode and sinogram projection data in the STIR library," *Physics in Medicine and Biology*, vol. 64, no. 3, p. 035 004, Jan. 2019.

[14] E. Ovtchinnikov *et al.*, "SIRF: Synergistic Image Reconstruction Framework," in *IEEE NSS-MIC*, IEEE, Oct. 2017, pp. 1–3.

[15] H. M. Hudson *et al.*, "Accelerated Image Reconstruction Using Ordered Subsets of Projection Data," *IEEE Transactions on Medical Imaging*, vol. 13, no. 4, pp. 601–609, 1994.

[16] K. M. Johnson *et al.*, "Optimized 3D ultrashort echo time pulmonary MRI," *Magnetic Resonoance in Medicine*, vol. 70, no. 15, pp. 1241–1250, 2013.

[17] M. Modat *et al.*, "Fast free-form deformation using graphics processing units," *Computer Methods and Programs in Biomedicine*, vol. 98, no. 3, pp. 278–284, 2010.

[18] R. Boellaard *et al.*, *FDG PET/CT: EANM procedure guidelines for tumour imaging: version 2.0*, 2015.